Journal of Hydrology 519 (2014) 2148–2164

Contents lists available at ScienceDirect

Journal of Hydrology

journal homepage: www.elsevier.com/locate/jhydrol

Water balance along a chain of tundra lakes: A 20-year isotopic perspective

J.J. Gibson [a,b,*], R. Reid [c]

[a] Alberta Innovates Technology Futures, 3-4476 Markham Street, Victoria, BC V8Z 7X8, Canada
[b] University of Victoria, Department of Geography, Victoria, BC V8W 3R4, Canada
[c] Aboriginal Affairs and Northern Development Canada, 3rd Floor, Bellanca Building, P.O. Box 1500, Yellowknife, NT X1A 2R3, Canada

ARTICLE INFO

Article history:
Received 26 October 2013
Received in revised form 17 September 2014
Accepted 4 October 2014
Available online 12 October 2014
This manuscript was handled by Laurent Charlet, Editor-in-Chief, with the assistance of Tamotsu Kozaki, Associate Editor

Keywords:
Isotopes
Arctic
Tundra
Chain lakes
Evaporation
Water balance

SUMMARY

Stable isotope measurements and isotope mass balance (IMB) calculations are presented in support of an unprecedented 20-year water balance assessment for a tailings pond and a chain of downstream lakes at the Salmita–Tundra mine site, situated near Courageous Lake, Northwest Territories, Canada (65°03′N; 111°11′W). The method is shown to provide a comprehensive annual and interannual perspective of water balance fluxes along a chain of lakes during the period 1991–2010, without the need for continuous streamflow gauging, and reveals important lake-order-dependent patterns of land-surface runoff, discharge accumulation, and several key diagnostic ratios, i.e., evaporation/inflow, evaporation/evapotranspiration, land-surface-runoff/precipitation and discharge/ precipitation. Lake evaporation is found to be a significant component of the water balance, accounting for between 26% and 32% of inflow to natural lakes and between 72% and 100% of inflow to mine-tailings ponds. Evaporation/evapotranspiration averages between 7% and 22% and is found to be higher in low-precipitation years, and in watersheds with a higher proportion of lakes. Runoff ratios for land-surface drainages and runoff ratios for watersheds (including lakes) ranged between 14–47% and 20–47%, respectively, and were higher in low precipitation years, in watersheds with a higher proportion of lakes, and in watersheds less affected by mining development. We propose that in general these two runoff ratios will likely converge as lake order increases and as land cover conditions become regionally representative. Notably, the study demonstrates application of IMB, validated with streamflow measurements, to constrain local water balance in a remote low-arctic region. For IMB chain-of-lakes applications, it underlines the importance of accounting for evaporatively-enriched upstream sources to avoid overestimation of evaporation losses.

1. Introduction

Isotope mass balance (IMB) using oxygen-18 and deuterium has been demonstrated as a useful approach for estimating water balance parameters of lakes (Gonfiantini, 1986; Gat, 1995), and has shown value particularly for assessments in remote regions such as the arctic and subarctic where baseline hydrologic data are limited (Birks and Gibson, 2009). While IMB results have been reported for dozens of large lakes around the world (see Jasechko et al., 2013), and for many small lakes, including those situated in the arctic and subarctic regions (Gibson and Edwards, 2002; Ichiyanagi et al., 2003; Leng and Anderson, 2003; Yi et al., 2008; Brock et al., 2009; Turner et al., 2010; Tondu et al., 2013; Anderson et al., 2013), few multi-year datasets have been compiled and interpreted (Lewis, 1979; Zimmerman, 1979; Hostetler and Benson, 1994; Sacks, 2002; Tyler et al., 2007; Longinelli et al., 2008). Multi-year datasets are often more informative as they capture seasonal and interannual variability in water balance and isotopic composition, which is especially important for cold-regions lakes subject to pulses of inflow during spring melt followed by short, seasonally-arid summers with high rates of evaporation (Gibson, 2002). This study presents a largely unpublished isotopic dataset spanning 20 years, from 1991 to 2010, based on weekly to monthly sampling during the thaw season, that provides new perspective on water balance variability over time along a chain of tundra lakes situated in the continental arctic of Canada.

IMB assessments carried out in northern Canada have commonly utilized steady-state methods to interpret spatial variability in isotope composition of lakes (e.g., Bursey et al., 1991; Gibson et al., 1993; Gibson and Edwards, 2002) and less commonly have

* Corresponding author at: Alberta Innovates Technology Futures, 3-4476 Markham Street, Victoria, BC V8Z 7X8, Canada. Tel.: +1 250 721 7341; fax: +1 250 483 1989.
E-mail address: jjgibson@uvic.ca (J.J. Gibson).

http://dx.doi.org/10.1016/j.jhydrol.2014.10.011
0022-1694/

applied non-steady-state methods to interpret data-intensive intervals of progressive seasonal enrichment (Gibson et al., 1996, 1998; Gibson, 2002; Gibson and Reid, 2010). With the exception of Gibson et al. (1998; six years) and Gibson and Reid (2010; 18 years) these investigations have been of limited duration. The latter study, developed in parallel with the present study, utilized isotopic variations in discharge from a chain-of-lakes watershed over an 18-year period to develop deeper understanding of inter-annual variability in evaporation losses, evaporation/evapotranspiration and partial contributing areas in a forested subarctic watershed near Yellowknife, Northwest Territories, Canada. The present study provides a 20-year perspective of water-balance variability along a chain of lakes situated at an abandoned mine site situated approximately 240 km northeast of Yellowknife, in close proximity to northern treeline. The results help to establish basic differences in hydrological response along a steep forest-tundra climatic gradient, which builds upon initial site assessments (Gibson, 2001) as well as knowledge gained from a regional survey of lakes across the region (Gibson and Edwards, 2002). Given that the region is remote and sparsely monitored, yet is undergoing rapid development for gold, base metals and diamond mining activities, details on the hydrological behavior of post-mining tailings ponds at the site also have particular relevance.

Improved understanding of modern stable isotope systematics in tundra lakes gleaned from this study may also inform interpretation of past records of lake-water isotopic variability as preserved in the lake sediments (Wolfe et al., 2007; Leng and Marshall, 2004). Our results may be particularly relevant for informing studies that use lakewater proxies to infer past hydrology and climate in the high-latitude cold regions (e.g. St. Amour et al., 2010; Edwards et al., 2004; Sauer et al., 2001).

In addition, this study offers insight into potential uncertainties associated with one-time isotopic surveys or short-term isotope-based assessments which may be incomplete due poor representation of seasonal and interannual variability. Overall, the system we examine serves as an example of a chain-of-lakes drainage that is less complicated than many around the world due to the presence of thick, continuous permafrost which limits surface–groundwater interaction. This natural simplification allows for quantitative application of IMB without detailed information on groundwater–lake exchanges.

The overall objectives of this paper are: (i) to describe the IMB model for a chain-of-lakes system; (ii) to present the 20-year isotopic dataset; (iii) to summarize the hydrological characteristics of the system as depicted by the IMB and establish a water balance for the site; (iv) to compare the method with available streamflow data; (v) to provide an assessment of evaporation from tailings ponds at the site; and (vi) to describe lake-order-dependent hydrological effects and identify avenues for future research.

1.1. Study site

The Salmita–Tundra gold mine (65°03′N; 111°11′W) is situated 240 km northeast of Yellowknife, Northwest Territories, Canada near the northern treeline (Fig. 1). The region is characterized by gently rolling tundra, low relief, and is underlain by PreCambrian bedrock, with a thin, discontinuous mantle of glacial till and numerous esker deposits. Lakes are abundant and drainage is disorganized. Salmita, now abandoned, was operated from 1983 to 1986, during which time mine tailings were placed in a small lake, now a tailings containment area (TCA), at the headwaters of a chain-of-lakes drainage. The site had been used previously during 1964–1968 to dispose of similar tailings from the nearby Tundra mine. Both tailings sources are rich in arsenic and other base metals which required isolation from natural waterways. When mining operations ceased at Salmita in 1986, the TCA was separated into an upper and lower pond (Fig. 1) with a dyke constructed from waste rock and esker material. The dyke was built to maintain a water cap over the bulk of the tailings solids located in the upper pond to limit the acid rock drainage potential. As a precaution, overflow culverts were installed to direct water to the lower pond. An interception ditch was also constructed on the north side of the tailings pond to minimize surface runoff to the lower pond. A waste-rock dam separates the lower pond from its downstream receiving waters, Hambone Lake, which subsequently drains into Powder Mag Lake and Sandy Lake on the way to Courageous Lake (Fig. 1). Sandy Lake also receives additional inflow from Trans Saddle Lake. Flow from the lower pond to Hambone Lake is predominantly via seepage through the waste-rock dam. Due to concerns about observed seepage, the dam was buttressed to reduce flows in 2004–2005 and water treatment and release began from the lower pond in 2009 as part of a plan to drain the ponds and establish a solid tailings cover beginning in 2014.

Mean annual temperature at the site is below zero, with mean air temperature during the evaporation season of 8.8 °C and relative humidity averaging close to 77%. On average there are 100–110 ice free days for most lakes. Outlets from small lakes are shallow (<1 m depth) and typically freeze to bottom in winter so that flow ceases for half the year. From observations in the mine workings, permafrost is known to be thick (several hundred metres) and continuous at the site. The relative position of the tailings ponds and string of lakes drainage network below the ponds is shown in Fig. 1.

2. Method

The application of the IMB technique for evaluating water balance requires information on the $\delta^{18}O$ and $\delta^{2}H$ composition of the lake water as well as measured climatology at the site (precipitation, temperature, relative humidity, evaporation and precipitation rates), geographic data (lake area, watershed area) and isotopic compositions of water balance components (mainly precipitation and water vapor). Our approach uses a steady-state approximation based on annually averaged data to capture interannual variability in evaporation losses and related water balance parameters. In this case, well-defined seasonal variations are useful as they help to constrain time-weighted averages of lake water isotopic composition in each year. The isotope mass balance methodology was previously described and demonstrated by Gibson and Reid (2010). A similar but more exact form of the balance equations is presented below.

2.1. Isotope mass balance

Basically, the IMB model determines evaporation/inflow ratio for each lake from the degree of offset between the measured isotopic composition of the water body and the estimated isotopic composition of inflow. Incorporating known precipitation and evaporation depth estimates then allows calculation of ungauged inflows to the lake (i.e. surface runoff plus active-layer inflows from the land surface) and the resultant outputs (evaporation and outflow). Additional water contributed by upstream lakes/reservoirs is also incorporated into the IMB. The theoretical basis of this model is explained further below.

In hydrologic and isotopic steady-state, water and isotope balances for a typical well-mixed lake or reservoir on an annual basis, are expressed, respectively as:

$$I = Q + E \quad (\mathrm{m}^3) \tag{1}$$

$$I\delta_I = Q\delta_Q + E\delta_E \quad (‰\,\mathrm{m}^3) \tag{2}$$

where I, Q and E are lake inflow, discharge and evaporation (m^3), and δ_I, δ_Q and δ_E are the isotopic compositions of inflow, discharge

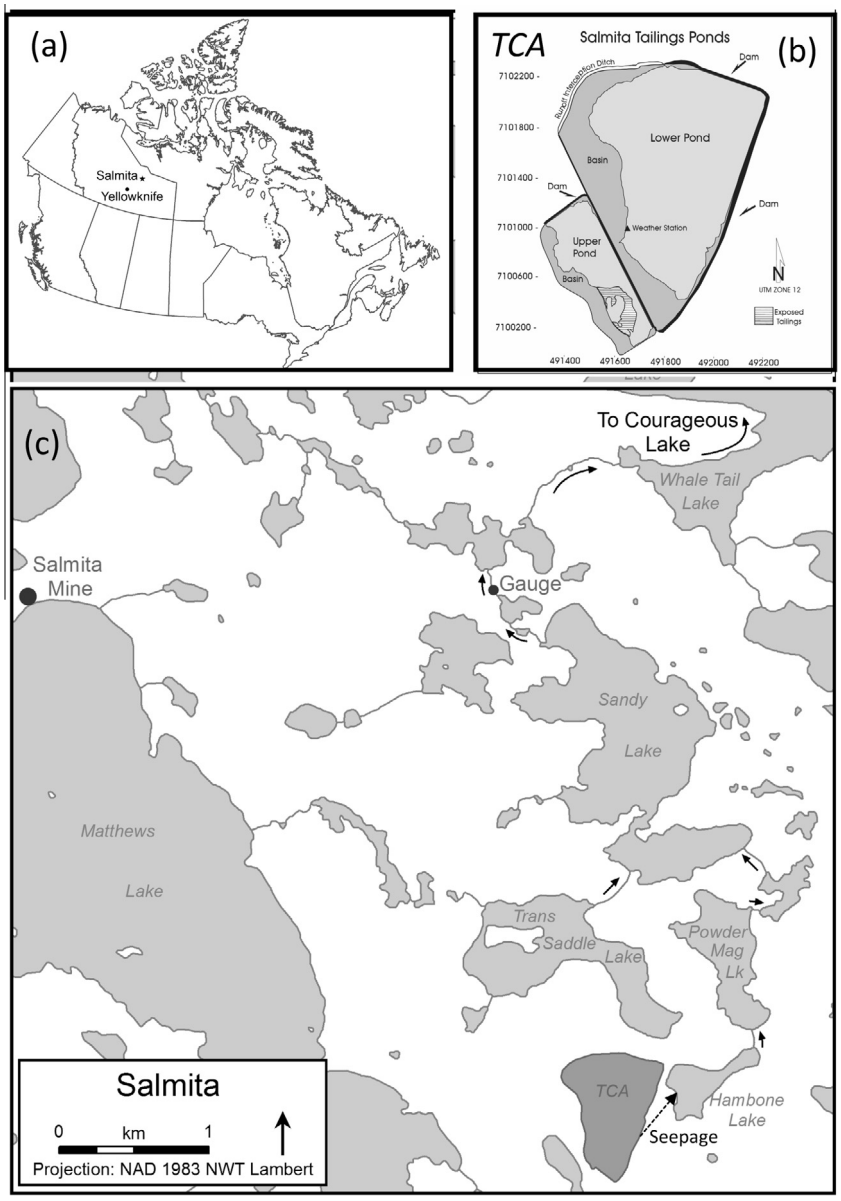

Fig. 1. Map showing (a) the locations of Salmita and Yellowknife, Northwest Territories, Canada, (b) the Salmita tailings containment area (TCA), consisting of the upper and lower pond, and (c) chain-of-lakes drainage network near Salmita, NT, also showing location of the TCA and Sandy Lake streamflow gauge. Arrows indicate channelized streamflow, and dashed line indicates seepage.

and evaporation fluxes (‰), respectively. Rearranging Eq. (2), and substituting $Q = I - E$ from Eq. (1) we obtain:

$$x = E/I = (\delta_I - \delta_Q)/(\delta_E - \delta_Q) \quad \text{(dimensionless)} \tag{3}$$

where x is the evaporation/inflow ratio. For well-mixed lakes it is apparent that $\delta_Q \approx \delta_L$ where δ_L is the isotopic composition of lake-water. While seasonal variation is characteristic in northern lakes, the steady-state isotope mass balance remains a useful description of the mean conditions of the lake water balance for each year. Lakes may receive input from precipitation on the lake, from surface/subsurface runoff, or from an upstream lake. This can be approximated by

$$I = P + R + J \quad (\mathrm{m}^3) \tag{4}$$

$$\delta_I = (P \cdot \delta_P + R \cdot \delta_R + J \cdot \delta_J)/(P + R + J) \quad (‰) \tag{5}$$

where P is precipitation on the lake (m^3), R is runoff (m^3), J is inflow from an upstream lake (m^3), and $\delta_P, \delta_R, \delta_J$ are the isotope compositions of precipitation, runoff and upstream lake water, respectively. Where evaporative enrichment of soil water is minor, as is often the case for tundra hillslopes (see Gibson et al., 1996), the isotope composition of runoff is similar to that of precipitation, i.e. $\delta_R \approx \delta_P$. For headwater lakes, the total inflow is therefore similar to precipitation, i.e., $\delta_I \approx \delta_P$.

The isotopic composition of evaporate δ_E can be estimated using the Craig and Gordon (1965) linear resistance model given by Gonfiantini (1986) as:

$$\delta_E = ((\delta_L - \varepsilon^+)/\alpha^+ - h\delta_A - \varepsilon_K)/(1 - h + 10^{-3} \cdot \varepsilon_K) \quad (‰) \tag{6}$$

where h is the relative humidity (decimal fraction), δ_A is the isotopic composition of atmospheric moisture, ε^+ is the equilibrium isotopic separation (see Horita and Wesolowski, 1994), α^+ is the equilibrium isotopic fractionation whereby $\varepsilon^+ = (\alpha^+ - 1) \cdot 1000$, and ε_K is the kinetic isotopic separation, the latter being quantified for

operational use from a range of laboratory and field experiments (see Horita et al., 2008). Substitution of δ_E into Eq. (3) yields:

$$x = E/I = (\delta_L - \delta_I)/(m(\delta^* - \delta_L)) \quad \text{(dimensionless)} \tag{7}$$

where

$$m = (h - 10^{-3} \cdot (\varepsilon_K + \varepsilon^+/\alpha^+))/(1 - h + 10^{-3} \cdot \varepsilon_K) \quad \text{(dimensionless)} \tag{8}$$

and

$$\delta^* = (h\delta_A + \varepsilon_K + \varepsilon^+/\alpha^+)/(h - 10^{-3} \cdot (\varepsilon_K + \varepsilon^+/\alpha^+)) \quad (‰) \tag{9}$$

Combining Eqs. (4) and (7), we can estimate R as:

$$R = E/x - P - J \quad (\mathrm{m}^3) \tag{10}$$

where $E = e \cdot LA$ and $P = p \cdot LA$; e and p representing the annual depth-equivalent of evaporation and precipitation (m), and LA being the lake area (m^2). The lake-evaporation/evapotranspiration ratio for the watershed can then be estimated by

$$E/ET = E/(E + T) = E/(E + P_R - R) \quad \text{(dimensionless)} \tag{11}$$

where T is vapor loss from the land-surface of the watershed (substantively transpiration) and $P_R = p \cdot DBA$ is precipitation on the land-surface of the watershed, DBA being the land-surface drainage area (not including the upstream lake basins). This calculation assumes no annual change in subsurface water storage. Runoff ratio can be estimated in two ways, as R/P_R representing runoff from land areas only, or as Q/P_W representing runoff from both land and lake areas; $P_W = p \cdot WA$ being the precipitation on the cumulative watershed upstream of the gauge, and WA being the watershed area.

The present analysis benefits from having a tailings pond (upper pond) at the site that approximates a terminal lake (see Gat, 1995), defined by $I = E$, where inflow is close to evaporation on a long-term basis. The pond has a limited catchment area, no surface outflow, and is underlain by permafrost that limits groundwater exchange. Applied as a 'terminal index lake' as suggested by Dincer (1968; see also Yi et al., 2008), the isotopic composition of this lake can be used to constrain the isotopic composition of local atmospheric moisture. When applying Eq. (7) for a terminal index lake we can substitute $x = 1$ to obtain an expression for the limiting isotopic enrichment (i.e. the maximum enrichment possible under local climatic conditions as water evaporates to dryness, see Gat, 1995):

$$\delta^* = (\delta_{TL}(1 + m) - \delta_{TL})/m \quad (‰) \tag{12}$$

where δ_{TL} is the isotopic composition of the terminal lake, from which, Eq. (9) can be rearranged to solve for the atmospheric moisture composition:

$$\delta_A = [\delta^*(h - 10^{-3}(\varepsilon_K + \varepsilon^+/\alpha^+)) - \varepsilon_K - \varepsilon^+/\alpha^+]/h \quad (‰) \tag{13}$$

This provides a calibration method for estimating δ^* (or δ_A) to apply Eq. (7) without long-term isotope measurements of the atmosphere. If the index lake has in fact leaked slightly (which is entirely possible at Salmita due to periodic overflows via culverts or by seepage to the lower pond), the derived inflow and outflow estimates need to be regarded as minimum values, which is still useful in the current application. Two other approaches are sometimes used to estimate δ_A. These include the assumption of isotopic equilibrium between mean annual precipitation and atmospheric moisture, i.e.:

$$\delta_A = (\delta_P - k\varepsilon^+)/(1 + 10^{-3} \cdot k\varepsilon^+) \quad (‰) \tag{14}$$

where $k = 1$ (see Gibson et al., 2008), or by fitting k to some fraction of 1 as a best-fit to the local evaporation line (see also Bennett et al., 2008). Later on, these approaches are also evaluated and compared with estimates based on the terminal lake method (Eq. (12)).

An IMB schematic for a typical chain of lakes is shown in Fig. 2. Fluxes are resolved in the series of lakes by simultaneous solution of the IMB equations for all lakes in the chain. The theoretical systematics of heavy isotope enrichment in such coupled evaporative systems has been previously described by Gat and Bowser (1991), although to our knowledge no previous applications have been demonstrated in the literature.

2.2. Watershed and climate parameters

Watershed areas (WA), drainage basin areas (DBA), and lake areas (LA) for each of the study lakes are summarized in Table 1.

The climatological parameters (precipitation, temperature, relative humidity, evaporation and precipitation rates) required to run the IMB model were obtained from direct measurements at the lower pond site (Table 2). The instrumentation at the site consisted

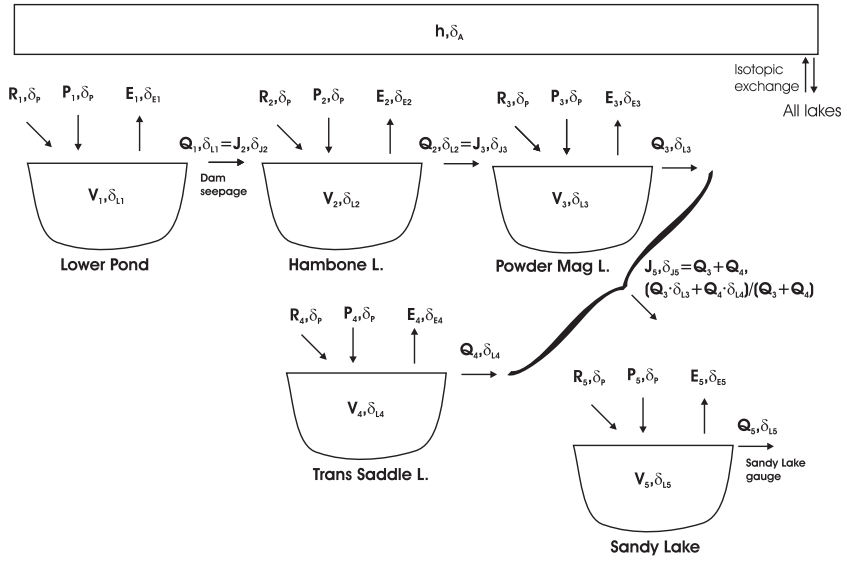

Fig. 2. Schematic depiction of the isotope mass balance for the chain of lakes drainage at Salmita. Note that relative humidity (h) and atmospheric moisture (δ_A) are assumed to be the same for all lakes. Note also that for lakes in series, outflow to the downstream lake is shown to be equal to inflow from the upstream lake. See text for discussion.

Table 1
Lake, drainage basin and watershed areas for the Salmita site. Pond areas are based on 1996 survey data.

Lake/pond	Lake area (m^2)	Drainage basin area (m^2)	Watershed area (m^2)
Upper pond	83,000	55,000	138,000
Lower pond	403,000	83,000	486,000
Hambone Lake	114,361	2,737,289	2,851,650
Powder Mag Lake	270,684	3,326,616	3,597,300
Sandy Lake	1,224,534	8,243,916	9,468,450
Trans Saddle Lake	542,674	1,264,976	1,807,650
Russell Lake[a]	353,121	1,819,479	2,172,600

[a] Prior to construction of tailings ponds.

of a tripod-mounted, automatic weather station located in shallow water at the edge of the lower tailings pond. Lower pond volume is estimated at 1.24×10^6 m^3. Air temperature, relative humidity and wind speed were measured at approximately 2.5 m above the water surface. Accuracy of the temperature and humidity sensors was ±0.2 °C and ±2–3%, respectively. Net solar radiation was measured at 1-m height and was used together with the wind speed, temperature and relative humidity data to estimate daily and annual evaporation by the Penman Combination method (see Reid and Faria, 2004). While it is acknowledged that seasonal timing of evaporation can vary significantly between large and small or shallow and deep reservoirs, estimates are considered to be representative of mean annual conditions for all lakes at the site. Precipitation was measured using both manual snow gauges and a tipping bucket rain gauge.

2.3. Water sampling

Water samples were collected in 30-mL high-density polyethylene bottles with minimal headspace and tightly sealed lids to minimize potential for evaporation. Procedures used for water sampling have been described previously (Gibson and Reid, 2010). In general grab samples of water were collected from the edge of the lake or pond during the ice-off period, rain samples were collected from an evaporation-free rain gauge, and snow was collected as depth-integrated grab samples. Note that use of grab samples to represent the whole water body presumes that the lakes/ponds were well-mixed and unstratified, which has been shown to be a reasonable approximation for many shallow northern lakes (Gibson et al., 2010). All isotope results are reported in δ notation in permil (‰) relative to Vienna Standard Mean Ocean Water (V-SMOW) and normalized to the SMOW-SLAP scale (see Coplen, 1996). We estimate analytical uncertainty to be better than ±0.2‰ for $\delta^{18}O$ and ±2‰ for δ^2H over the past 20 years.

3. Results and discussion

3.1. Isotope characteristics

Isotope data for natural lakes and tailings ponds plot below the Global Meteoric Water Line (GMWL) in δ^2H–$\delta^{18}O$ space (Fig. 3a and b) which is typical for evaporating water bodies sampled in the region and across northern Canada (Gibson et al., 2005). Evaporation line slopes are found to be fairly consistent, ranging from about 5.3 for the lower pond, 5.5 for the upper pond and about 5.6 for three natural lakes. Degree of offset below the GMWL along evaporation lines is proportionate to the fraction of water loss by evaporation from each lake or reservoir, with seasonality in inflow and evaporation rates contributing to variability in the degree of offset. A few class-A evaporation pan measurements also attest to the potential for evaporative enrichment at the site during the thaw season (Fig. 3a). Rain samples are shown to plot along a line with a slope of 6.3, slightly below the GMWL (Fig. 3c), which is common for rain sampled across Canada, as reported by the Canadian Network for Isotopes in Precipitation (Birks and Gibson, 2009). Snow plots closer to the GMWL which is similar to that observed from a larger snow dataset collected near Yellowknife as part of the Baker Creek watershed studies (see Gibson and Reid, 2010; their Fig. 3). Seepage water, found in abundant pools along the base of lower pond dams, is also shown in comparison with the lower pond (i.e. the primary seepage source) and rain/snow (Fig. 3c). Seepage water is found to plot close to the lower pond line but there may also be minor mixing occurring between pond water and precipitation or active layer water sources as the seepage exfiltrates the pond. The mean isotopic composition of precipitation δ_P is estimated to be −22‰ for $\delta^{18}O$ and −166‰ for

Table 2
Average meteorological conditions during the study including thaw season temperature, relative humidity, evaporation and annual precipitation. Isotope data include limiting isotopic enrichment and atmospheric moisture composition calculated from the index lake. δ^*_{18} and δ^*_2 are $\delta^{18}O$ and δ^2H, respectively, of limiting isotopic enrichment based on Eq. (12); δ_{A18} and δ_{A2} are oxygen and hydrogen isotopic compositions of atmospheric moisture based on Eq. (13).

Year	T (°C)	h (dimensionless)	p (mm)	e (mm)	δ^*_{18} (‰)	δ^*_2 (‰)	δ_{A18} (‰)	δ_{A2} (‰)
1991	7.2	0.77	–	–	−12.98	−119.4	−31.36	−241.6
1992	5.0	0.79	–	–	−12.30	−119.1	−29.80	−236.8
1993	5.8	0.78	218	279	−12.16	−116.1	−29.26	−226.8
1994	11.2	0.67	213	336	−9.39	−101.4	−32.05	−240.4
1995	7.5	0.74	266	261	−11.13	−111.0	−30.10	−230.4
1996	10.4	0.78	269	283	−11.62	−112.9	−29.48	−233.6
1997	5.1	0.79	260	243	−13.58	−122.8	−30.75	−235.7
1998	8.6	0.75	283	348	−10.09	−98.9	−29.21	−226.3
1999	5.2	0.78	289	295	−12.39	−110.9	−30.07	−230.0
2000	6.0	0.78	270	278	−12.76	−120.3	−30.46	−238.4
2001	6.1	0.81	302	296	−12.71	−116.1	−29.43	−232.5
2002	4.4	0.80	307	232	−12.84	−119.0	−29.30	−229.0
2003	9.1	0.77	231	327	−11.69	−112.8	−30.34	−239.5
2004	2.8	0.78	224	242	−11.02	−112.7	−29.11	−236.9
2005	2.9	0.78	244	235	−11.80	−117.2	−29.46	−234.2
2006	7.3	0.75	385	340	−11.95	−113.3	−31.10	−239.7
2007	4.8	0.76	237	222	−12.37	−116.0	−30.04	−228.6
2008	11.5	0.75	315	251	−12.32	−115.8	−31.11	−236.5
2009	8.1	0.78	178	219	−12.38	−114.5	−29.31	−223.3
2010	12.5	0.75	172	273	−10.92	−105.4	−30.77	−241.5
Mean	7.1	0.77	259	276	−11.92	−113.8	−30.13	−234.1

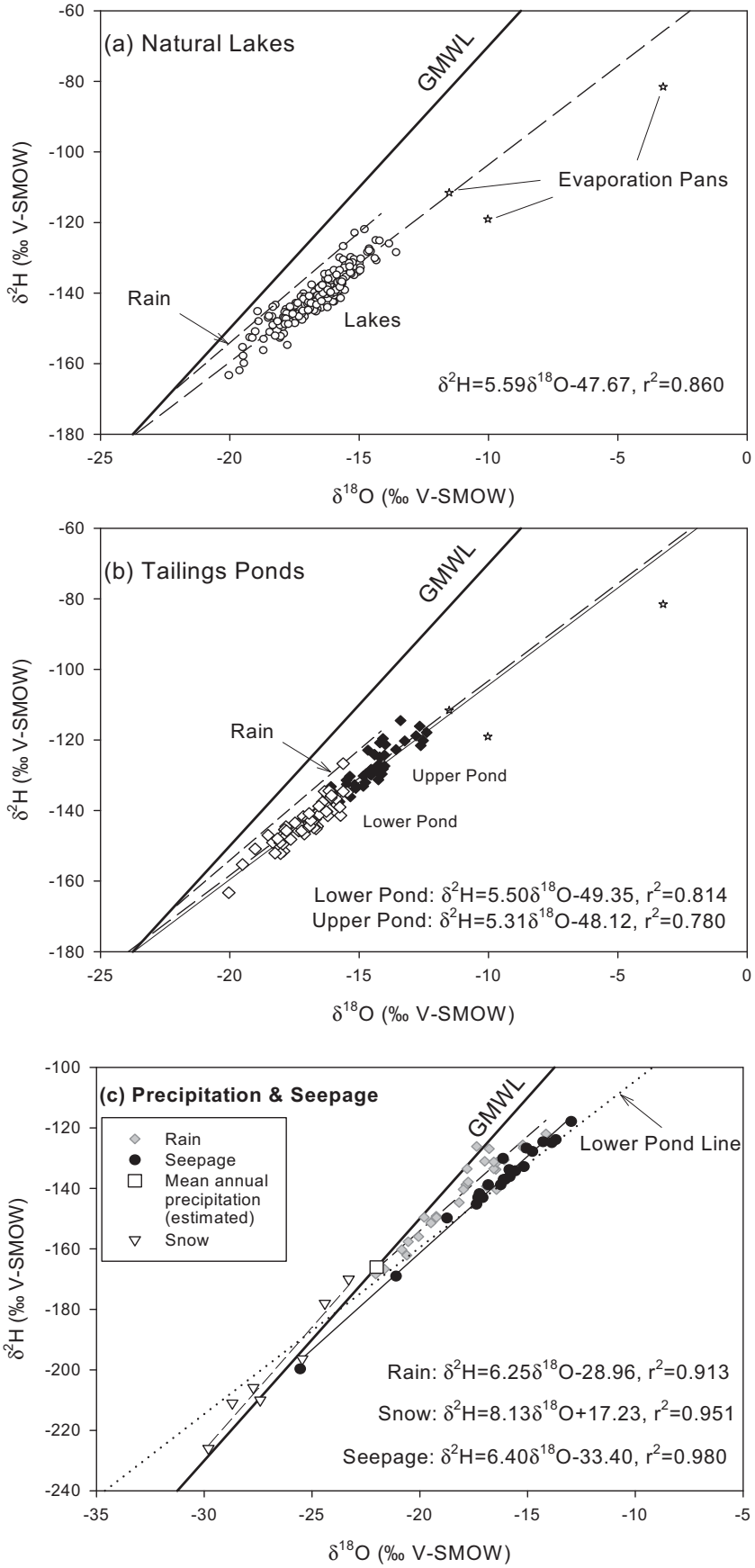

Fig. 3. δ^2H–$\delta^{18}O$ plots of (a) natural lakes, (b) tailings ponds, and (c) precipitation and seepage. GMWL denotes the Global Meteoric Water Line of Craig (1961) given by $\delta^2H = 8\delta^{18}O + 10$. Regressions in (a) and (b) illustrate the apparent slope of local evaporation lines for selected lake(s)/reservoir. Estimated mean annual isotopic composition of precipitation is also shown.

δ^2H (see also Gibson, 2001), reflecting the approximate balance between rain and snow at the site, and this roughly coincides with the intercept of the rain line and GMWL (Fig. 3c).

Time-series of δ^{18}O in the upper and lower tailings ponds, and in Hambone, Powder Mag and Sandy Lakes (Fig. 4) illustrates the systematic seasonal cycles of evaporative enrichment from early to late thaw season. This strong cyclicity is enhanced by abundant inflow of snowmelt that is isotopically depleted during the freshet and arid conditions during the summer that promotes isotopic enrichment by evaporation. Typical seasonal variations at Salmita are in the range of 2–4‰ in δ^{18}O (20–40‰ for δ^2H). Similar cycles have been shown for sites north and south of Salmita (i.e. Gibson

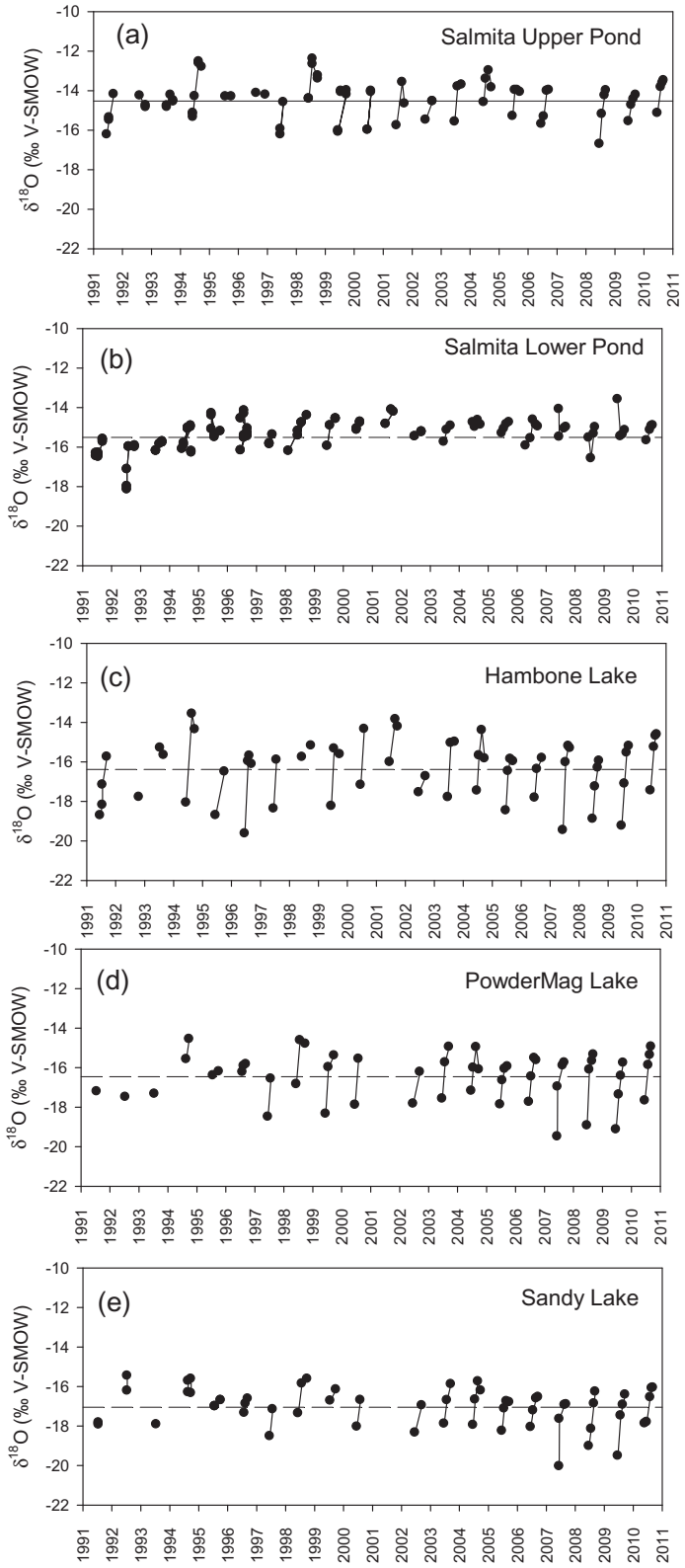

Fig. 4. Time-series of δ^{18}O for lakes and tailings ponds at Salmita, NT, illustrating both seasonal enrichment over individual thaw seasons (points joined by lines) and long-term patterns.

et al., 1996, 1998; Gibson and Reid, 2010). Interannual variations in the degree of enrichment (maxima and minima in Table 3) correspond to shifts along the local evaporation lines. Nearly identical isotopic composition of lake water was observed in Powder Mag Lake (PM) and Trans Saddle Lake (TS) during 1991–1996, which yielded the regression: $\delta^{18}O_{TS} = 1.0\delta^{18}O_{PM} - 0.01$; $r^2 = 0.97$; $n = 7$. Sampling of Trans Saddle Lake was discontinued after 1996.

Isotopic composition of key water balance components are shown relative to GMWL and the predicted slope of the LEL in Fig. 5. Note that the range of values for inflow (δ_I) arises from blending of upstream lake water with precipitation, and is different for each lake in each year. Values for δ_A and corresponding δ^* (Table 2) are shown for the index lake based on Eqs. (13) and (12), respectively, and compared to two values of δ_A based on equilibrium and best-fit assumptions using Eq. (14) (Fig. 5). Ranges in the index lake values reflect annual differences in both δ_L and in meteorological conditions in each year, whereas ranges in δ_A for the other methods reflect variations in meteorological conditions alone. Mean lake water values plot slightly below the predicted evaporation line slope for the area suggesting slightly greater influence of snowmelt on these lakes than the tailings ponds.

3.2. Calculations

A series of calculations are made, based on the equations presented in Section 2.1, to illustrate the potential for quantitative application of the IMB method for describing interannual water balance variations. For each year, the basic IMB scenario developed for the Salmita lake chain (Fig. 2) assumes isotopic and hydrologic steady-state, i.e. constant values for volume and δ_L for each lake, and for all lakes, a common δ_A based on Eq. (13), and using a temperature and relative humidity representative of the evaporation season. The watersheds are assumed to be underlain by continuous permafrost so that liquid outflows are exclusively via channelized streamflow without significant groundwater losses. Inflow from the land surface is assumed to be via surface or shallow active-layer pathways. A constant value for δ_P, equal to the mean annual precipitation, is used in all years, which is a simplification required due to lack of year-to-year data for amount-weighted precipitation, but one that appropriately takes into account the longer-term buffering role of runoff (R), which is presumed to be derived largely from displacement of longer-term active-layer storage by precipitation recharge. Such old water sources have been noted to be significant even in arctic and subarctic watersheds (Carey and Quinton, 2005; Ombradovic and Sklash, 1986). This water accounts on average for 70–80% of $P + R$ to the Salmita lakes.

Before running the isotope mass balance, lake evaporation (E) and precipitation (P) were estimated for each lake based on micro-meteorological estimates of e and p (see Table 2). Then, for each year, evaporation/inflow (x) and land-surface runoff (R) were estimated for each lake using Eqs. (7) and (10), respectively. Note that upstream lake inflow (J) was estimated iteratively using Eqs. (4) and (5). Initially, a first order approximation of the lake water balances were calculated using $J = 0$ and $\delta_I = \delta_P$. These estimates of J and the proportion of $J/(P + R + J)$ were then used in subsequent iterations to converge on a best fit value for both J and δ_I for each lake in each year. Q was then calculated as a residual.

Table 3
Summary of isotope composition of lakes and ponds. σ_{18} and σ_2 are standard deviations of mean annual isotopic composition for $\delta^{18}O$ and δ^2H, respectively.

Lake/reservoir	Mean		Maximum Annual		Minimum Annual		Mean seasonal variability		
	$\delta^{18}O$	δ^2H	$\delta^{18}O$	δ^2H	$\delta^{18}O$	δ^2H	σ_{18}	σ_2	n
Upper pond	−14.55	−128.7	−13.42	−119.5	−15.58	−134.1	0.74	4.20	20
Lower pond	−15.30	−133.0	−14.39	−128.4	−16.73	−143.6	0.47	2.57	20
Hambone L.	−16.37	−139.6	−14.69	−128.0	−17.78	−154.7	1.44	8.04	20
Powder Mag L.	−15.70	−143.1	−15.07	−129.1	−17.50	−157.8	1.12	4.44	20
Sandy L.	−16.24	−143.5	−15.84	−135.3	−17.92	−151.5	0.79	4.60	20

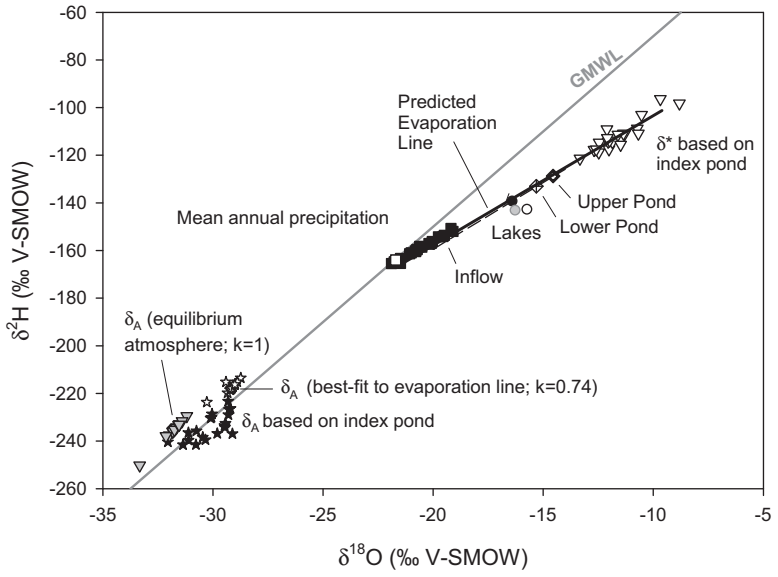

Fig. 5. δ^2H–$\delta^{18}O$ plot showing mean isotopic compositions of the upper pond, lower pond and lakes, as well as annual inflows, atmospheric moisture composition, and limiting isotopic enrichment. The lake symbols are the same as in Fig. 6. Dashed line is the local evaporation line based on regression; solid line is the predicted local evaporation line.

The IMB was computed slightly differently for Sandy Lake. To account for dual inflows, water balances were computed and Q values were estimated and summed from both Powder Mag and Trans Saddle, the upstream lakes (see Fig. 2). The Trans Saddle lake isotope mass balance was computed using the Powder Mag isotopic record and the regression noted above but assuming no upstream lakes.

The operational value of using IMB is that land-surface runoff and discharge can be simultaneously calculated for a lake, as compared to a conventional water balance where only one unknown can be calculated. The value of application to a chain of lakes is that discharge from the upstream lake can be used to characterize the upstream inflows to the next lake in the chain, thereby refining the calculation. Overall, the water balance estimates provide an isotopic perspective of the integrated hydrology of the lake-watershed systems, and capture the downstream propagation of water from the headwaters to the Sandy Lake outflow.

Two additional isotope-based water balance partitions are also evaluated. E/ET is estimated based on Eq. (11) and runoff ratio is estimated in two ways, as Q/P_W and R/P_R. These quantities are used to demonstrate some basic hydrologic properties of the chain of lakes and to illustrate comparisons between Salmita and the Baker Creek watershed situated 240 km to the southwest near Yellowknife, Northwest Territories, Canada.

Prior to presenting the results it is important to establish the intrinsic role of the upper pond as an index lake. The upper pond was chosen to serve as an index lake because its long-term water balance was close to that of a terminal lake, i.e. $I = E$; $Q = 0$. Suitability of the pond as an index lake was initially recognized due to its physical attributes, i.e., limited catchment, lack of surface outflow, and permafrost substrate. This hypothesis was reinforced by the approximate balance between local e and p (see Table 2), and then by the close agreement between δ_A estimated from Eq. (13) and using the best-fit method from Eq. (14) (Fig. 5). While this overall site assessment might have adopted the best-fit approach for estimating atmospheric moisture, as did Gibson and Reid (2010), the use of the index method was selected as it resulted in slightly higher calculated x and reduced discharge from the lower pond, which is a better match to observed outflow that occurred only as slow seepage. While the upper pond underwent minor seasonal changes in volume and significant seasonal enrichment in isotope composition similar to other lakes (Fig. 4), only annual averages were used in the computations. Slight leakage from the reservoir is suggested by records of winter water levels which were typically stable to slightly declining (~0.1–0.3 m) over the course of the season. Probable volume of seepage in winter is likely in the range of 12,000–25,000 m^3, or between 2.5% and 5% of the upper pond volume.

Under a scenario where the upper pond may be leaking slightly (<5%) we anticipate that our water balance will tend to overestimate x in the lower pond by up to 10% and underestimate outflows by a similar amount. Owing to less overall enrichment in the natural lakes, potential overestimation of x and underestimation of outflow for these water bodies is limited to about 3%.

Table 5
Spearman Rank correlation matrix for water balance fluxes and selected indicator ratios for Sandy Lake. The correlation coefficient (r), p value (p), and number of samples (n) is shown for each. Note that significant correlations are bolded and shaded.

		E	*R*	*J*	*Q*	*x*	*R/P*	*Q/P*	*E/ET*
P	*r*	0.289	−0.057	−0.025	0.0281	0.21	**−0.686**	**−0.57**	**−0.774**
	p	0.213	0.809	0.917	0.905	0.381	**0.001**	**0.011**	**<0.001**
	n	20	19	19	19	19	**19**	**19**	**17**
E	*r*		0.065	0.03	−0.144	**0.641**	−0.232	−0.408	−0.102
	p		0.787	0.9	0.55	**0.003**	0.334	0.082	0.687
	n		19	19	19	**19**	19	19	17
R	*r*			0.454	**0.912**	**−0.63**	**0.714**	**0.711**	0.429
	p			0.05	**<0.001**	**0.004**	**<0.001**	**<0.001**	0.083
	n			19	**19**	**19**	**19**	**19**	17
J	*r*				**0.596**	−0.318	0.288	**0.495**	0.15
	p				**0.007**	0.181	0.227	**0.031**	0.559
	n				**19**	19	19	**19**	17
Q	*r*					**−0.789**	**0.614**	**0.7**	0.299
	p					**<0.001**	**0.005**	**<0.001**	0.237
	n					**19**	**19**	**19**	17
x	*r*						**−0.653**	**−0.758**	−0.287
	p						**0.002**	**<0.001**	0.258
	n						**19**	**19**	17
R/P	*r*							**0.932**	**0.863**
	p							**<0.001**	**<0.001**
	n							**19**	**17**
Q/P	*r*								**0.716**
	p								**<0.001**
	n								**17**

Results from the isotope mass balance model calculations, as shown in Tables 4–6 and Figs. 6–9, are discussed in the following sections.

3.3. Evaporation/inflow

Evaporation/inflow (or its reciprocal) is a commonly-used throughput indicator in IMB investigations of open-water bodies as it relates directly to the degree of isotopic enrichment of the water bodies above background levels found in precipitation and groundwater (see Gat and Levy, 1978; Gibson, 2002). Whereas evaporation/inflow (x) is ~1 for Salmita's upper pond 'index lake', x is estimated to be significantly less than 1 for the lower tailings pond and much lower for natural lakes along the chain (Table 4; Fig 6). This implies that all have significant inflows and outflows, which is consistent with observations. Mean values of x were computed as the average of $\delta^{18}O$ and $\delta^{2}H$ values for each reservoir in each year. As shown (Table 4), $\delta^{18}O$- and $\delta^{2}H$-based estimates differed on average by 4%, 12%, 23% and 4% for the lower pond,

Table 4
Summary of evaporation/inflow, evaporation/evapotranspiration and runoff ratios based on isotope mass balance ±1σ interannual variability.

Lake/reservoir	x (for ^{18}O)	x (for ^{2}H)	Mean x	E/ET	R/P_R	Q/P_W
Upper pond	–	–	~1	–	–	–
Lower pond	0.73 ± 0.21	0.70 ± 0.16	0.72 ± 0.18	–	3.2 ± 3.3	0.47 ± 0.45
Hambone L.	0.34 ± 0.18	0.30 ± 0.13	0.32 ± 0.16	0.071 ± 0.061	0.14 ± 0.12	0.20 ± 0.18
Powder Mag L.	0.31 ± 0.07	0.24 ± 0.13	0.28 ± 0.09	0.13 ± 0.05	0.25 ± 0.13	0.34 ± 0.20
Sandy L.	0.27 ± 0.07	0.26 ± 0.09	0.26 ± 0.08	0.22 ± 0.09	0.47 ± 0.18	0.47 ± 0.18
Trans Saddle L.[a]	–		~0.36	–	–	~0.65

[a] Approximate only – based on Powder Mag isotope record.

Hambone Lake, Powder Mag Lake and Sandy Lake, respectively, which reflects the goodness of fit of each lake water balance to the overall isotope mass balance scenario shown in Fig. 2.

Mean x ($\pm 1\sigma$) is 72% (±18%) for the lower pond, 32% (±16%) for Hambone Lake, 28% (±9%) for Powder Mag Lake and 26% (±8%) for Sandy Lake. While x is found to decrease down the chain of lakes, interannual variability in x, as given by the standard deviation from year-to-year, is found to dampen from 18% to 6% down the chain of lakes (Table 4). The same general pattern holds true for Trans Saddle Lake and Sandy Lake although the former is based on a more limited dataset. Due to higher liquid throughput in successive lakes, we postulate that this is how the stable isotope signature of a water parcel might typically respond as it moves down a series of evaporating reservoirs in an arctic climate zone with continuous permafrost. Temporal patterns in x are fairly similar for all natural lakes (Fig. 6), with minimum values observed in 1991–1992 and maximum values observed in 1994 and 2000–2001 (the latter for Hambone Lake only). A different temporal pattern for the lower pond suggests some alteration of natural evaporation and runoff in this artificial reservoir. It is important to note that x would have been overestimated by between 30% and 50% if enriched water from upstream lakes was not incorporated into the model. For both modern and paleohydrology applications, this emphasizes the importance of determining the position of the lakes in the chain of lakes and sampling the upstream sources.

For Sandy Lake, based on a Spearman Rank correlation (Table 5), we find that x is positively correlated with evaporation rate e ($r = 0.641$, $p = 0.003$), which might be expected given that both are controlled by lake evaporation, and negatively correlated with discharge (Q) ($r = -0.789$, $p < 0.001$) and land-surface runoff (R) ($r = -0.63$, $p = 0.004$) which is also expected as these fluxes drive increased throughput. Similar results are found for the other natural lakes. Spearman Rank correlations are used throughout this paper due to non-normal distribution of parameters R and x.

3.4. Interannual water balance of lakes

A summary of water balance fluxes for the chain of lakes (in $m^3\ yr^{-1}$) is shown in Fig. 7 and summarized in Table 6. As E and P are estimated using equivalent depths of evaporation and precipitation, variations in these fluxes among lakes is strictly attributed to differences in the surface area of each lake. Note that average values for the study period were used to characterize P in 1991 and 1992 and E in 1991–1993 prior to comprehensive annual precipitation surveys and complete evaporation season monitoring at the site. Of the water fluxes, both J and Q are shown to increase down the chain of lakes, primarily reflecting accumulation of water, whereas R varies with the land-surface area of the respective catchments. Temporal trends are dominated by significant peaks in upstream inflow in all lakes in 1992 and by peaks in runoff and discharge in 1993. Lowest values of runoff and discharge are noted in 1992 and 1994. The peaks noted in upstream inflow in 1992 may be an artifact of a poor representation of precipitation amount in this year, although there is no obvious reason why runoff and discharge are predicted to have been so much higher for 1993. The remainder of the record, extending from 1994 to 2010 is characterized by more consistent outputs for all water balance fluxes, and this period is thought to be more representative of average water balance conditions of the lakes.

Gauging of the Sandy Lake outflow was carried out during 2006–2010 and provides some insight into the overall performance of the isotope mass balance model (Fig. 7). During the open-water season, cumulative discharge estimates for the Sandy Lake outflow based on standard physical gauging methods ranged from $7.7 \times 10^5\ m^3$ in 2006 to $1.4 \times 10^6\ m^3$ in 2008 and 2009, which is in broad agreement with mean isotope mass balance estimates of discharge from Sandy Lake ($1.2 \times 10^6 \pm 0.35 \times 10^6\ m^3\ yr^{-1}$). This lends general confidence to the chain-of-lakes IMB scenario. Note that P (estimated from meteorological data) contributes to about 20% of this discharge, whereas R and J (both estimated isotopically) contribute 60% and 20%, respectively.

Gibson and Reid (2010) noted two general water-climate periods for the Baker Creek watershed near Yellowknife: a drier period during 1991–2000, and a wetter period during 2001–2008. According to the Climate Trends and Variations Bulletin of Canada 2012 (Environment Canada, 2013) the Mackenzie District experienced above-average precipitation as compared to the 1961–1990 normal in only 5 of 10 years during 1991–2000 and in 9 of 10 years during 2001–2010, suggesting a similar regional pattern to that noted for Baker Creek. No distinct wet (1990s) and dry (2000s) periods are noted for Salmita. Interestingly, for 18 of 20 study years, temperature was also above 1961–1990 normals in the Mackenzie District (Environment Canada, 2013). Due to lack of a reliable historical weather record at Salmita it is difficult to judge whether the site follows the regional temperature trend, but slight warming is indicated by the 1991–2010 temperature record.

From a Spearman Rank correlation analysis for Sandy Lake (Table 5) we find that P and E are not significantly correlated with each other or with any other water balance fluxes, but that Q is highly correlated with R ($r = 0.912$, $p < 0.001$) and moderately correlated with J ($r = 0.596$, $p = 0.007$). The high correlation between R and Q is expected given that R is a measure of water runoff from land areas of the watershed whereas Q is a measure of runoff from both land and water areas. Correlation between Q and J is also anticipated given that these both reflect lake outflows along the chain. Lack of correlation between Q and P reveals that year-to-year variations in precipitation on the lake are not influential in determining the interannual variations in basin outflow. Similar results are found for the other natural lakes.

3.5. Evapotranspiration and vapor flux partitioning

It is interesting to note that lake evaporation, while an important process, is not the dominant evapotranspiration mechanism,

Table 6
Summary of water balance results $\pm 1\sigma$ interannual variability ($\times 10^3\ m^3\ yr^{-1}$).

Lake/pond	P[a]	E[b]	J[c]	R[c]	Total inflow[a,c] $P+R+J$	Q[c]
Upper pond	21.6	22.9	0	1.3	22.9	0
Lower pond	105 ± 19.8	111 ± 15.8	~0	63.8 ± 66.2	169 ± 63.2	57.4 ± 54.8
Hambone L.	29.8 ± 5.6	31.7 ± 4.5	57.4 ± 54.9	94.2 ± 81.5	181 ± 130	135 ± 125
Powder Mag L.	70.0 ± 13.4	74.7 ± 10.9	142 ± 125	217 ± 77.2	429 ± 179	317 ± 165
Sandy L.	317 ± 60.6	338 ± 49.1	317 ± 165	1040 ± 327	1672 ± 353	1176 ± 353
Trans Saddle L.[d]	140	149	~0	298	438	289

[a] Measured.
[b] Based on Penman method.
[c] Based on isotope balance.
[d] Approximate only, based on limited dataset.

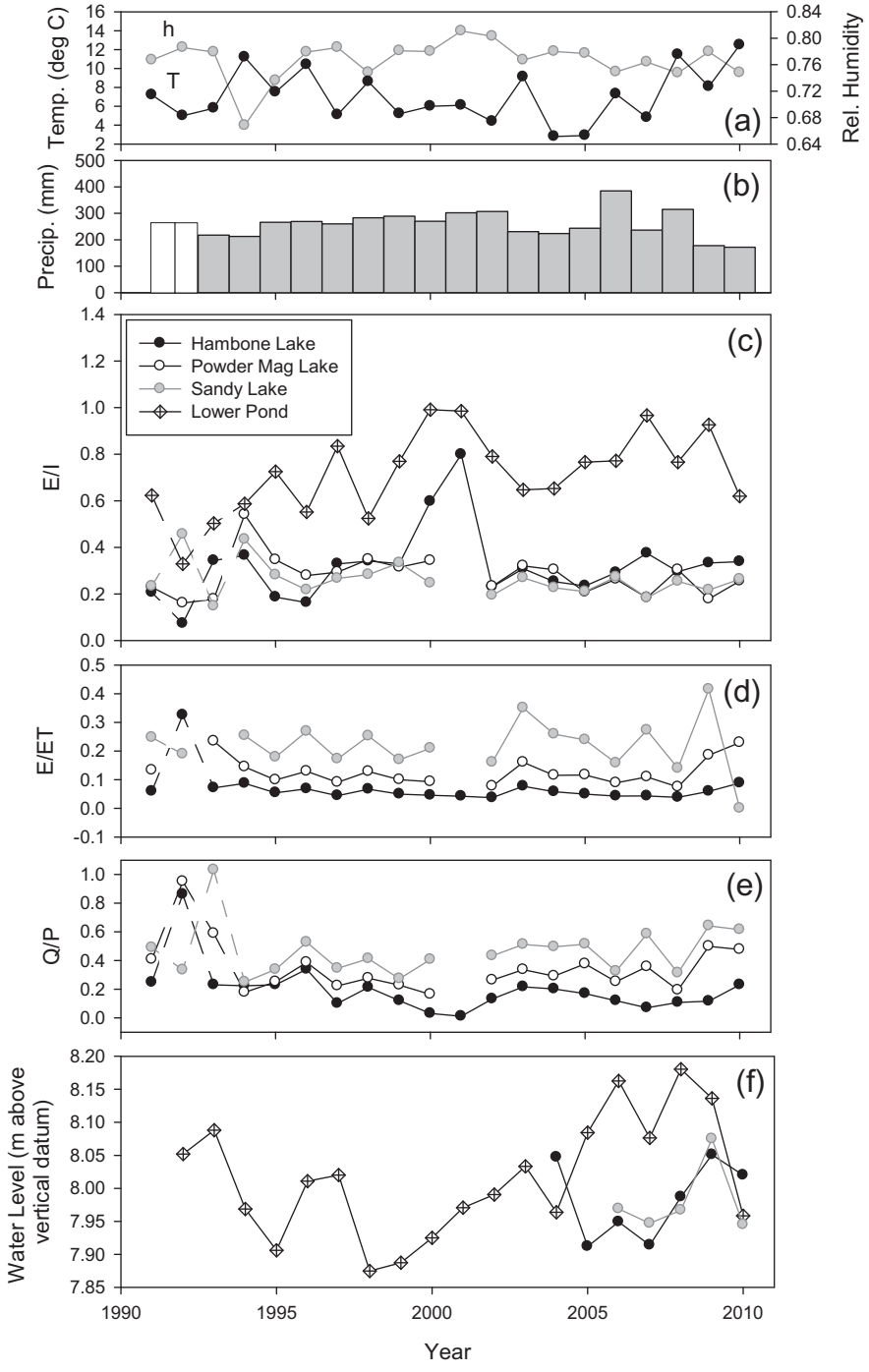

Fig. 6. Temporal trends in (a) annual temperature and humidity, (b) annual precipitation, and isotope-based hydrologic indicators, including: (c) evaporation/inflow, (d) lake-evaporation/evapotranspiration, (e) runoff ratio for the watersheds, and (d) available water levels. Note that dashed lines denote the interval during 1991–1993 when annual precipitation was not recorded. Open bars in (b) denote precipitation estimates based on mean annual values.

evapotranspiration from land surfaces being greater. Overall, *E*/*ET* for watersheds of Hambone Lake, Powder Mag Lake and Sandy Lake is estimated at 7% (±6%), 13% (±5%) and 22% (±9%), respectively. Based on Spearman Rank correlation analysis (Table 5), *E*/*ET* for the Sandy Lake watershed is found to be negatively correlated with *P* ($r = -0.774$, $p < 0.001$). Similar results are noted for the other natural lakes. Note that no significant correlation is found between *E*/*ET* and any of the water balance fluxes or with *x* suggesting that these are distinct indicators, but both *E*/*I* and *E*/*ET* show co-dependence with the runoff ratios (see Table 5). The relationship between precipitation and *E*/*ET* for natural lakes is illustrated in Fig. 8a.

In general, the *E*/*ET* ratio is found to decrease in higher precipitation years, a finding which might arise from reduced land–lake sensible heat advection under wetter conditions. In this situation, evaporation from the lakes may be reduced during years when the land is also wet due to reduction in atmospheric transport of sensible heat from the land to the lake. Likewise, *E*/*ET* can be expected to increase in low precipitation years as land-to-lake sensible heat advection increases due to a higher contrast in dry land and wet lake surfaces (see McNaughton, 1976; Bello and Smith, 1990).

Partitioning results are also plotted from Baker Creek near Yellowknife for 1991–2008, which reveals the dominance of vapor loss by lake evaporation in a subarctic shield watershed with

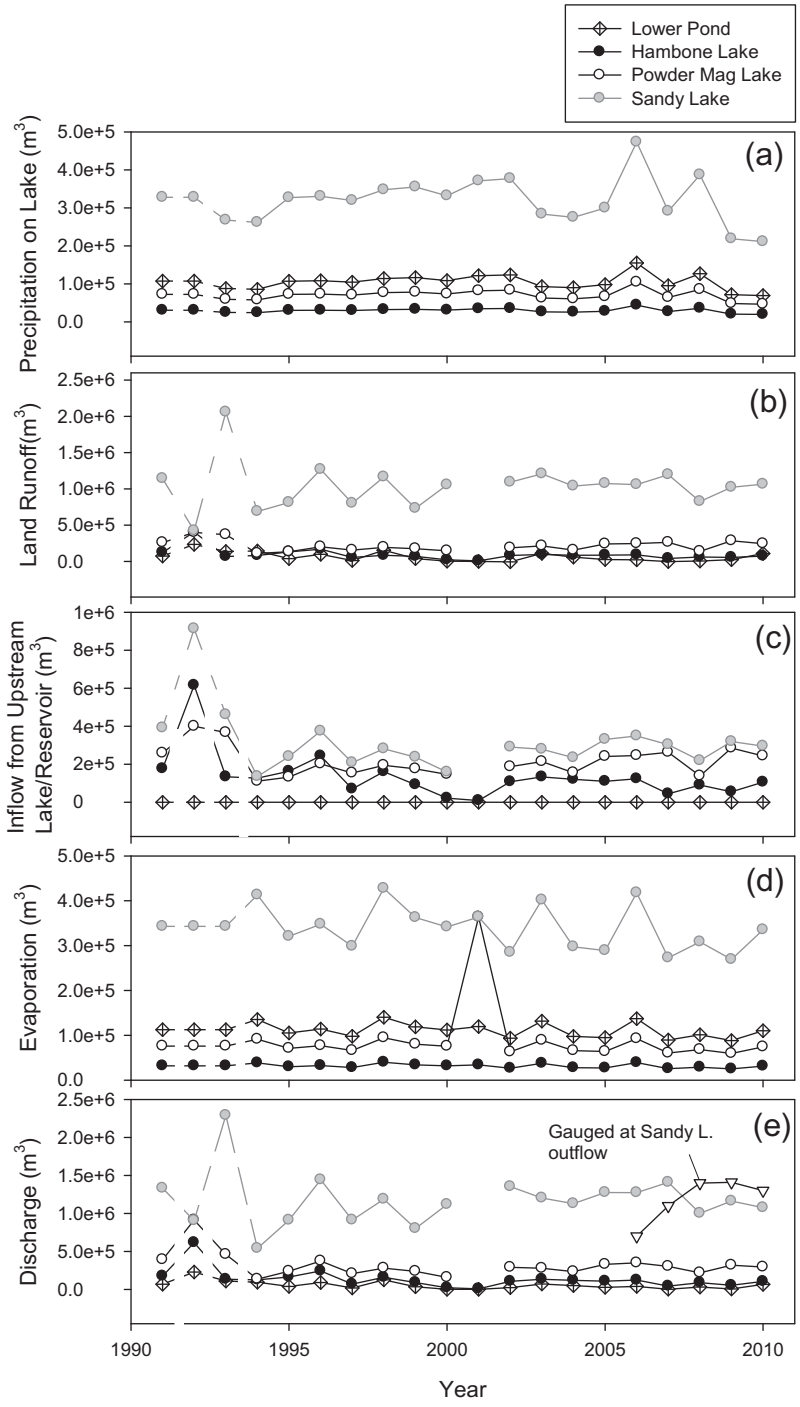

Fig. 7. Water balance fluxes for the lower pond and natural lakes (a) precipitation on lake (b) land-surface runoff, (c) inflow from upstream lake/pond, (d) evaporation, and (e) discharge. Note that average values are used for precipitation and evaporation in 1991 and 1992 prior to complete evaporation-season monitoring at the site.

discontinuous permafrost and 21% lake cover (Fig. 8a). Note that the Baker Creek watershed is distinct from watersheds at Salmita in that it comprises hundreds of lakes and has a significantly variable effective drainage area depending on antecedent moisture conditions. Effective drainage area is defined as the area of the watershed that is connected at any given time to the outlet stream. As Baker Creek is a chain-of-lakes drainage, disconnections between lakes along the chain has a significant impact on the effective drainage area (see Spence et al., 2010). In fact E/ET shows a stronger correlation with effective drainage area ($r^2 = 0.71$, $p < 0.001$; Gibson and Reid, 2010) than with precipitation at Baker Creek. By comparison, the effective drainage area of the Salmita watersheds is not typically variable as the lakes are normally continuously connected during the thaw season. E/ET is also significantly higher on average for Baker Creek, especially under drier conditions when the watershed becomes partially disconnected and the effective percentage of lake area increases above 21%. At Salmita, E/ET is found to be higher for Sandy Lake with a lake/watershed ratio of 14% as compared to 8% for Powder Mag Lake and 4% for Hambone Lake.

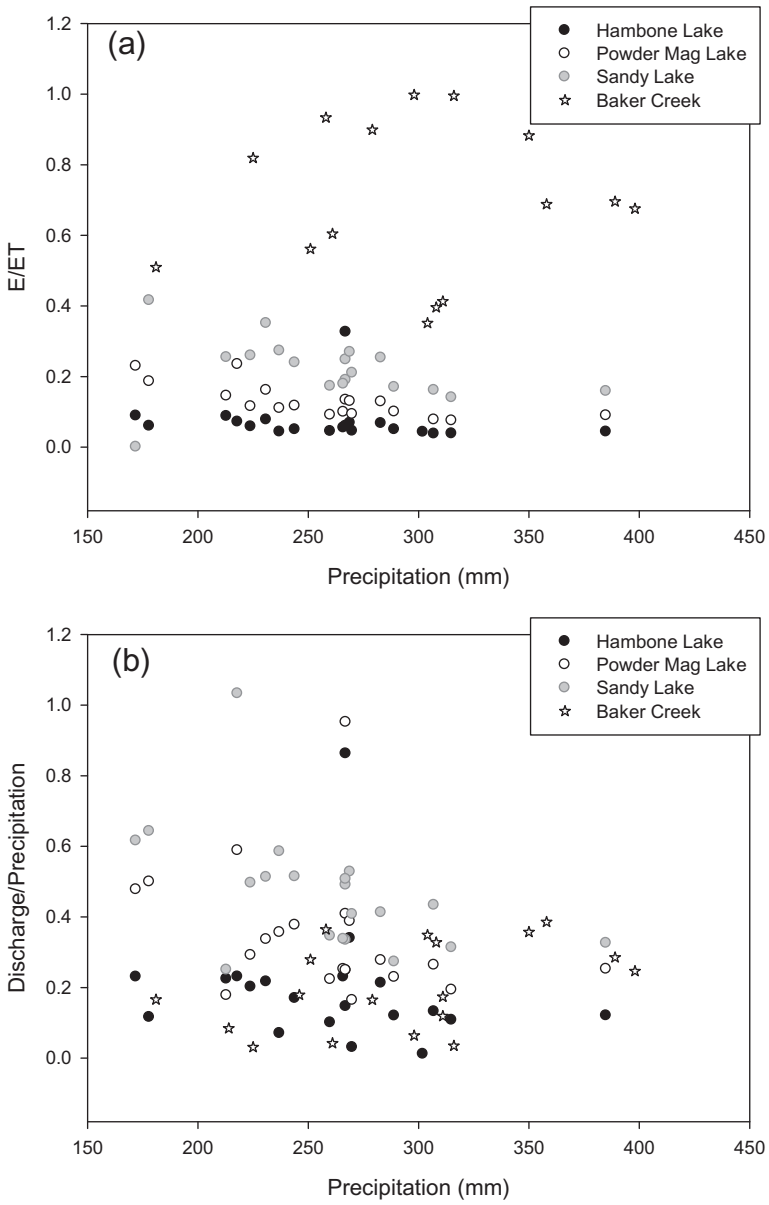

Fig. 8. Crossplots of (a) annual lake-evaporation/evapotranspiration, and (b) annual watershed runoff ratios versus precipitation. Annual values are also shown for the Baker Creek watershed, a subarctic Shield watershed located near Yellowknife (from Gibson and Reid, 2010).

3.6. Runoff and runoff ratio

Depth of runoff (also termed specific discharge) from the natural watersheds was estimated to be 51 ± 47 mm yr^{-1} for Hambone Lake, 88 ± 46 mm yr^{-1} for Powder Mag Lake, and 116 ± 35 mm yr^{-1} for Sandy Lake (Table 7). Increasing runoff depths down the chain of lakes (and an overall reduction in variability) appears to be systematic, and is directly correlated with lake area and watershed area. In a study of specific discharge for 80 undisturbed boreal catchments ranging from 0.12 to 67 km^2, Lyon et al. (2012) reported reduced variability with watershed area, especially above 10 km^2, and a positive correlation between specific discharge and percentage of wet area (i.e., wetlands, mires, lakes). Given that the Sandy Lake watershed is slightly less than 9.5 km^2 and lakes tend to be larger as lake order increases, we expect that variability at Salmita may further decrease as water passes through subsequent lakes (Whale Tail and Courageous Lake), and that eventually the specific discharge will become representative of the regional runoff. While results from Sandy Lake are likely more regionally representative than the other lakes, we emphasize that specific discharge, at least in catchments less than 9.5 km^2, appears to be lake-order-dependent.

Runoff ratios, calculated both as R/P_R (i.e. land-surface runoff) and Q/P_W (land + lake runoff) also increase down the chain of lakes, varying from 14 ± 12% to 47 ± 18% for R/P_R and 20 ± 18% to 47 ± 18% for Q/P_W (Table 4). As expected, Q/P_W for Sandy Lake is strongly correlated with R/P_R ($r = 0.932$, $p < 0.001$) and Q ($r = 0.701$, $p < 0.001$), and negatively correlated with P ($r = -0.57$, $p = 0.011$). Comparable trends are found for the other natural lakes. Interestingly, the difference between R/P_R and Q/P_W is reduced as lake order increases, and these values converge for Sandy Lake. We propose that convergence on a runoff ratio of 47 ± 18%, which we attribute to similarity of wet area percentages between the two footprints (i.e., land only versus land + lake area for Sandy Lake), likely suggests that this runoff ratio may be approaching a stable value that is areally representative for the region. Lyon et al. (2012) demonstrated this to occur between about 10 km^2 and 67 km^2 in a boreal watershed with a large number of lakes.

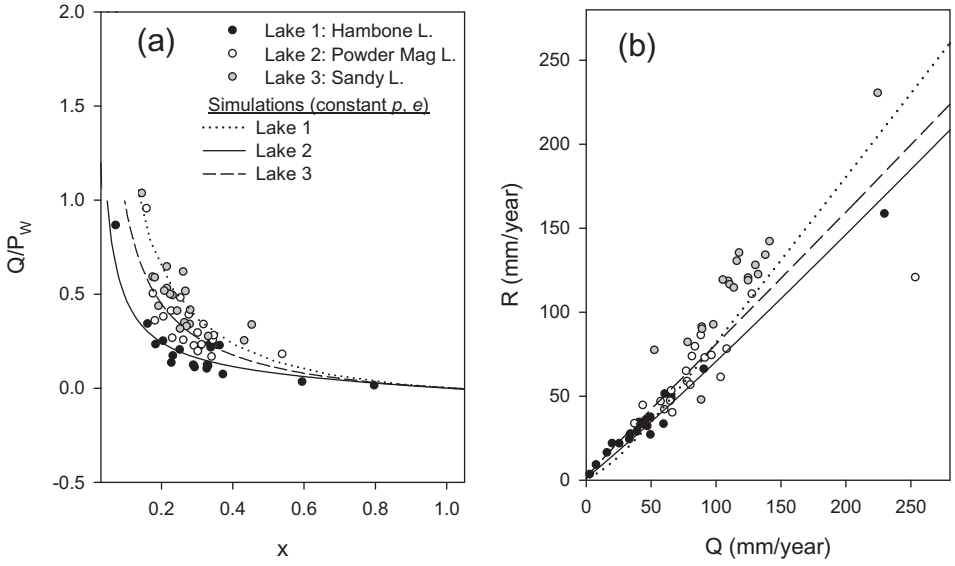

Fig. 9. Plots illustrating IMB response, including: (a) watershed-runoff/precipitation versus evaporation/inflow, and (b) landscape runoff versus lake outflow. Data points are calculated annual values for lakes, 1990–2010; lines represent simulated response for a range of potential water balance conditions, with precipitation and evaporation rates held constant and equal to mean observed values. *R* is runoff from land surfaces to the lake; *Q* is outflow from the lake.

Similar to *E*/*ET*, runoff ratios are found to be greater in dry years as compared to wet years, although this is driven predominantly by reduction in *P* rather than by increase in *Q* (or *R*) (Fig. 8b). We also speculate that release of active-layer storage (i.e. old water; see Ombradovic and Sklash, 1986) plays a larger buffering role relative to precipitation in dry years, augmenting the runoff ratios, although this was not confirmed through detailed measurements. The importance of land surface storage was also noted by FitzGibbon and Dunne (1981) for a lake-rich tundra/lichen woodland with discontinuous permafrost near Schefferville, Quebec, although surficial depression and detention storage rather than active layer storage were thought to be the primary runoff sources. Situated in discontinuous permafrost terrain at 62.4°N, the Baker Creek watershed near Yellowknife was found to have a mean annual runoff ratio of 20 ± 12% based on 18 years of isotope-based data (Gibson and Reid, 2010). For Baker Creek there is no significant correlation between runoff ratio and precipitation (Fig. 8b), largely because of the complicating influence of variations in effective drainage area. To our knowledge, no other studies at northern high latitudes have examined evolution of runoff ratios along a chain of lakes drainage. Rather, with some exceptions (e.g. Spence et al., 2010) most of the site-specific studies conducted to date have targeted headwater drainage basins. Using isotope-based methods at Salmita, we find an increase in the long-term annual runoff ratio (Table 4) over short distances along a string of tundra lakes.

One essential caveat in our study, which affects mainly the two upstream lake water balances, is that runoff and runoff ratios may be reduced to some extent by mining and tailings pond development, activities that are designed to capture runoff. Given that the tailings area accounts for approximately 22%, 17% and 7% of the watershed areas of Hambone, Powder Mag and Sandy Lakes, respectively, we suggest that these percentages likely bracket the effective alteration of the natural runoff processes. Our attempts to directly characterize the lower-pond land-surface areas resulted in runoff ratios of between 47% and 320% (Table 4). These ratios are high to impossible given that disturbance is expected to reduce rather than enhance runoff in the current setting, as dams and ponds impound and restrict water outflow. We suspect that our delineated drainage area and watershed area for the TCA are significantly too small, possibly as a result of poor performance of the interception ditch that was assumed to divert water from the northern boundary of the TCA to Trans Saddle Lake, and this has elevated the apparent runoff ratio. Note that *R* and *Q* calculated from IMB for the lower pond are not affected by this, only the runoff ratio diagnostic.

3.7. Integrated water balance

A major finding of this study is that the Salmita water balance parameters (Table 7) are found to be within the expected range for watersheds in northern high latitudes given latitude, mean annual precipitation, and permafrost conditions as shown by Kane and Yang (2004) in a synthesis of water balance results from thirty-nine experimental watersheds located in the northern high latitudes, including sites in Russia, Finland, Norway, Greenland,

Table 7
Summary of areally-weighted watershed fluxes (mm·yr^{-1}) for Salmita compared to previous studies. Note that Sandy Lake is likely more representative of the regional conditions.

Basin/characteristics	Precip.	Evap.	Transp.	Discharge
This study				
Hambone L. Lake/Land × 100 = 5%22% developed	259 ± 52	12 ± 2	197 ± 66	51 ± 47
Powder Mag L. Lake/Land × 100 = 8%17% developed	259 ± 52	21 ± 3	157 ± 55	88 ± 46
Sandy L. Lake/Land × 100 = 13% 7% developed	259 ± 52	33 ± 5	111 ± 58	116 ± 35
Gibson and Reid (2010)				
Subarctic forest Lake/Land × 100 = 21% variably connected	292 ± 59	200 ± 66	46 ± 33	62 ± 44
Gibson and Edwards (2002)				
Near Treeline, modal water balance	325	40	160	125
Subarctic forest, modal water balance	340	60	240	40

Japan, Canada and the United States. Mean annual precipitation at Salmita is estimated to be 259 ± 52 mm yr^{-1}, similar in magnitude to Wolf Creek, Yukon Territories, Canada (61°N), and subarctic/arctic sites at higher latitude such as Havikpak Creek (68.3°N) and Trail Valley Creeks (68.7°N) near Inuvik, Northwest Territories, Canada (see Kane and Yang, 2004). Evapotranspiration, which ranged from 144 ± 57 to 209 ± 66 mm yr^{-1} for Salmita, is similar in magnitude to that reported for Havikpak Creek, C2 catchment (Caribou and Poker Creeks Watersheds), located in the Alaskan interior (65.2°N), and Upper Kuparuk and Imnavait Creek, located on the North Slope, Alaska (68.6°N). ET/P at Salmita is found to range from 54 ± 15% to 80 ± 18%, similar in proportion to C2 and C4 catchments in the Alaskan Interior (65.2°N) (Kane and Yang, 2004).

The global average runoff ratio is reported as 36% (Baumgartner and Reichel, 1972). Kane and Yang (2004) show that annual runoff ratios in the high-latitude experimental watersheds are latitude-dependent, varying generally from between about 0 and 25% at 50–55°N to between 80% and 125% at 70–80°N, with a range of 20–75% at 60–70°N. At Salmita (65°N), runoff ratio was found to range from 20% to 47%, within the range observed in the 60–70°N latitude band, and similar to C2, C3 and C4 catchments, located in the Alaskan Interior, and Havikpak Creek near Inuvik, Northwest Territories, Canada (Kane and Yang, 2004). Spatially, the pattern observed at high-latitude sites is toward higher runoff ratios at sites with lower precipitation and more extensive permafrost, although year-to-year response at individual sites is normally toward higher runoff ratios in wet years, possibly due to larger contributing areas. At Salmita, we detect higher runoff ratios with lower precipitation totals but on an interannual basis, although the driver of this behavior may be active layer interaction as noted in previous isotope-based investigations in discontinuous to continuous permafrost where 'old water', water present in the basin prior to snowmelt, was estimated to account for more than half of overall streamflow (Ombradovic and Sklash, 1986; Carey and Quinton, 2005). Ombradovic and Sklash (1986) found that 60% of annual streamflow in a continuous permafrost catchment on southern Baffin Island consisted of water that was present in the catchment prior to snowmelt. Our isotope mass balance results also imply a significant proportion of active layer interaction at Salmita.

One limitation of conventional studies, as summarized by Kane and Yang (2004), has been that they provide no information on the relative partitioning of ET into its component fluxes. Water balance results, including an ET partitioning summary are compared with previous isotope-based evaluations by Gibson and Edwards (2002), who estimated spatial distribution of x and E/ET in the Salmita region based on a survey of 255 lakes (Table 7). For lakes located within 50 km of the northern treeline, Gibson and Edwards (2002) reported x values ranging from near zero to ~35% and E/ET in the range of 5–35%. Results from Salmita fall on the high end of this range for E/I and within the range for E/ET. Given that the survey focused on non-headwater lakes and targeted lakes equal to or larger than Sandy Lake, we conclude that the survey was more representative of conditions in higher-order lakes. This evidence suggests that the water balance may continue to evolve toward lower x and higher runoff along the chain of lakes at Salmita downstream of the study lakes.

Compared to Gibson and Reid (2010) we find that the proportion of water losses by evaporation and transpiration at Salmita are almost reversed as compared to Baker Creek which, in the latter, is driven largely by disconnection of upstream lakes from the main drainage stem. This makes evaporation losses more important in the connected portion of the watershed linked to the outflow stream. Note that the isotopic signal, and hence the water balance for Baker Creek, is not representative of the areal losses from the topographically-defined watershed but rather of the connected portion of the watershed. The isotopic method applied to discharge provides no information on the disconnected areas. Compared to distributions presented by Gibson and Edwards (2002), Baker Creek appears to be an example of a more evaporative system, although not uncommon in the area. Key processes that drive the hydrologic balance in the forest–tundra transition are degree of connectivity of chain-of-lakes drainages, and evolution of water balance along the chain of lakes.

3.8. Model systematics

We conclude the discussion with an overview of several key water balance patterns revealed by the model. The most striking feature of the modelled outputs is the lake-order effect, i.e., the systematic evolution of lake and watershed balances along the chain of lakes. A plot of runoff ratio (Q/P_W) versus x (Fig. 9a) illustrates the IMB depiction of the exponential runoff response of the watersheds, as driven by temporal variations of throughput in the system. As x approaches unity (i.e., terminal lake) the annual runoff ratio from the watersheds approaches zero, whereas as x approaches zero, runoff ratio increases exponentially (Fig. 9a). Generation of runoff components from similar exponential expressions has been widely used in serial reservoir cascade models (Cheng, 2010). Interannual variations in runoff ratio during the 20-year period are found to span the full range of Q/P_W from greater than one ($x \sim 0.1$, high throughput) to near zero ($x \sim 0.8$, low throughput). For the Salmita chain of lakes, a progressively higher range of Q/P_W (and R/P_R) is associated with increasing lake order (Fig. 9a). This is attributed to increase in lake area (and also wet areas of the land surface) which promotes runoff, and to successively lower rates of lake flushing as lake size increases along the chain. We propose in general that runoff ratios will continue to evolve down a chain of lakes until land cover characteristics become regionally representative. While, as noted, convergence of R/P_R and Q/P_W may be an early indication of areal representativeness for Sandy Lake, survey data from Gibson and Edwards (2002) may suggest that water balance continues to evolve significantly. Their survey data appear to indicate that larger lakes with more depleted isotopic signatures and lower x are most abundant in the lower drainage networks near the northern treeline and extending to the north.

As shown in Fig. 9b, a linear correlation is found between land surface runoff and lake discharge (see also Table 5 statistics for Sandy Lake). We note that correlations between R and Q, and the other water balance fluxes, are lake-specific and lake-order-dependent. Both from regressions of annual data, and a series of simulations with constant p and e (see lines, Fig. 9b) we find that R and Q generally evolve to become more equal along the lake chain as lake order increases. We are unaware of previous studies that have documented this effect.

4. Conclusions and implications

Water balance information is scarce across the northern high latitudes, particularly in this sparsely populated region of the continental arctic which is under rapid development for mining of gold, base metals and diamonds. Results of this 20-year study therefore offer a significant contribution to understanding of water balance conditions in the region, and represent one of two studies of its kind and duration (Gibson and Reid, 2010 being the other) carried out in the Arctic drainage basin. While the IMB method was effectively applied to characterize the interannual variability in the major water cycle fluxes in a chain of tundra lakes, we note that it was not very effective at directly capturing the role of storage of water on land and in lakes. An obvious improvement to the IMB as applied would be to incorporate lake level and active layer

monitoring (of both water level and isotopic composition) as demonstrated in previous isotope mass balance studies (e.g. Gibson et al., 1996), although this was not possible due to limited time during infrequent visits to the site, particularly during the 1990s when funding for the study was more limited. This would be especially important in order to utilize the model for sub-annual time scales. Indirectly, the method may be capable of detecting the buffering effect of active layer storage on the catchment runoff in low-precipitation years.

This study provides the first comprehensive record of seasonal and interannual variability in isotopic composition of lakes in a continental arctic watershed in North America, and describes evolution of isotopic signals along a chain of lakes. One important implication is the need for caution when interpreting isotopic data from short-term sampling campaigns, either site-specific lake evaluations or regional assessments, due to temporal variability. We find that a single late July/early August sampling time would have been most representative of average conditions at Salmita for three lakes less than 1.2 km^2 in area, and this is consistent with the timing of the Gibson and Edwards (2002) survey. However, repeat sampling at more than one time of year, or in subsequent years, as demonstrated by Gibson and Edwards (2002; see also Turner et al., 2010; Tondu et al., 2013), lends greater confidence to the results.

Isotope systematics established from this study have two main implications: (i) that isotopic composition of upstream inflow may be required to accurately determine the isotope mass balance of a non-headwater lake and, (ii) given the pronounced seasonal variability of lake water isotopic composition in arctic environments, that sediment archives of lake water isotopic composition such as aquatic cellulose should be interpreted cautiously, as they may have been formed outside of the late July/early August interval when the lake water isotopic composition is most representative of the mean open-water period. This will lead to bias, albeit a systematic one, in quantitative interpretation of the isotopic record which needs to be reconciled in paleohydrologic or paleoclimatic reconstructions.

Several conclusions can be drawn from the study of the Salmita tailings ponds. The lower pond lost an estimated 72% of its water by evaporation and the upper pond lost close to 100%. This suggests that ponds were more effective evaporators than natural lakes, but that tailings ponds were still likely to generate outflow and hence were not effective as a total containment strategy for arsenic and heavy metal contamination. Observed seepage suggests that the pond was in a non-sustainable long-term situation. Radically higher runoff ratios calculated for the lower pond (Table 4) may indicate that water sources above the interception ditch are also contributing runoff to the pond. We suspect that the effective drainage area is at least four times larger than predicted, but smaller than the original catchment of the pre-existing lake. Observed seepage, estimated to account for less than 5% of the volume of the lower pond, and gauging at the Sandy Lake outflow serve usefully to constrain the isotope mass balance presented here. One interesting utility of the isotope mass balance perspective for mine-waste management in the region is that it may be possible without extensive gauging to predict the effective dilution of acid-mine drainage at different levels of the downstream receiving waters. It may also be useful for simulating long-term conditions prior to pond development or after pond removal.

Finally, the Salmita study demonstrates the capability of isotope-based methods to characterize the water balance of tundra lakes, and illustrates some of the advantages of using the approach to develop a long-term perspective on water budget without extensive instrumentation requirements. This is especially valuable for hydrologic observation programs in remote, ungauged or poorly instrumented regions. It is important to note that concurrent physical monitoring of streamflow, lake water levels, active-layer water levels, frost tables, runoff, and land-surface evapotranspiration is recommended where possible to ground-truth isotope-based methods or potentially to calibrate or refine the approach for operational use. Ideally, physical gauging should be used periodically to verify the isotope mass balance fluxes, as was done for several years at Salmita. Overall, this study demonstrates a feasible methodology for application of isotope-mass balance to multi-lake systems as a contribution to the hydrological toolkit, and puts into practice some of the important coupled evaporative reservoir concepts posited by pioneers such as Gat and Bowser (1991). It is important also to note that isotope mass balance methods have limitations, as they are dependent on representativeness of sampling, and assumptions regarding mixing and isotopic and hydrologic steady-state. Nevertheless, in terms of research impact, some of the most productive future applications may be in defining hydrologic drivers of lake-ecosystem processes and biogeochemistry in studies of regional lake organization, similar to that reported by Soranno et al. (1999).

Acknowledgements

Funding for this research was provided by Water Resources Division, Aboriginal Affairs and Northern Development Canada and the Natural Sciences and Engineering Research Council of Canada. This manuscript benefited from insightful discussions with Dr. Yi Yi, AITF. Dr. T.W.D. Edwards and three anonymous reviewers also provided informative comments that helped to improve upon earlier versions of this manuscript.

References

Anderson, L., Birks, S.J., Rover, J., Guldager, N., 2013. Controls on recent Alaskan lake changes identified from water isotopes and remote sensing. Geophys. Res. Lett. 40, 1–6.

Baumgartner, A., Reichel, E., 1972. The World Water Balance. Elsevier, New York, USA, 179 p.

Bello, R., Smith, J.D., 1990. The effect of weather variability on the energy balance of a lake in the Hudson Bay Lowlands, Canada. Arct. Alp. Res. 22, 98–107.

Bennett, K.E., Gibson, J.J., McEachern, P.M., 2008. Water yield estimates for critical loadings assessment: comparisons of gauging methods versus and isotopic approach. Can. J. Fish. Aquat. Sci. 65, 83–99.

Birks, S.J., Gibson, J.J., 2009. Isotope hydrology research in Canada, 2003–2007. Can. Water Resour. J. 34 (2), 163–176.

Brock, B.E., Yi, Y., Clogg-Wright, K.P., Edwards, T.W.D., Wolfe, B.B., 2009. Multi-year landscape-scale assessment of lakewater balances in the Slave River Delta, NWT, using water isotope tracers. J. Hydrol. 379, 81–91.

Bursey, G.G., Edwards, T.W.D., Frape, S.K., 1991. Water balance and geochemistry studies in a tundra watershed, district of Keewatin, Northwest Territories. In: Prowse, T.D., Ommanney, S.S.L. (Eds.), Northern Hydrology: Selected Perspectives, NHRI Symposium No. 6. Saskatoon, Saskatchewan, pp. 17–31.

Carey, S.K., Quinton, W.L., 2005. Evaluating runoff generation during summer using hydrometric, stable isotope and hydrochemical methods in a discontinuous permafrost alpine catchment. Hydrol. Process. 19, 95–114.

Cheng, S.-J., 2010. Generation of runoff components from exponential expressions of serial reservoirs. Water Resour. Manage. 24, 3561–3590. http://dx.doi.org/10.1007/s11269-010-9621-0.

Coplen, T.B., 1996. New guidelines for reporting stable hydrogen, carbon, and oxygen isotope-ratio data. Geochim. Cosmochim. Acta 60, 3359–3360.

Craig, H., 1961. Isotopic variations in meteoric waters. Science 133, 1702–1703.

Craig, H., Gordon, 1965. Deuterium and oxygen-18 in the ocean and marine atmosphere. In: Tongiorgi, E. (Ed.), Stable Isotopes in Oceanographic Studies and Paleotemperatures. Spoleto, Italy, pp. 9–130.

Dincer, T., 1968. The use of oxygen-18 and deuterium concentrations in the water balance of lakes. Water Resour. Res. 4, 1289–1306.

Edwards, T.W.D., Wolfe, B.B., Gibson, J.J., Hammarlund, D., 2004. Use of water isotope tracers in high-latitude hydrology and paleohydrology. In: Pienitz, R., Douglas, M.S.V., Smol, J.P. (Eds.), Long-term Environmental Change in Arctic and Antarctic Lakes. Springer, Netherlands, pp. 187–207 (Chapter 7).

Environment Canada, 2013. Climate Trends and Variations Bulletin. Annual 2012. <http://www.ec.gc.ca/adsc-cmda/default.asp?lang=En&n=77842065-1> (retrieved 12.10.13).

FitzGibbon, J.E., Dunne, T., 1981. Land surface and lake storage during snowmelt runoff in a subarctic drainage system. Arct. Alp. Res. 13, 277–285.

Gat, J.R., 1995. Stable isotopes of fresh and saline lakes. In: Lerman, A., Imboden, D., Gat, J. (Eds.), Physics and Chemistry of Lakes. Springer-Verlag, New York, pp. 139–166.

Gat, J.R., Bowser, C.J., 1991. Heavy isotope enrichment in coupled evaporative systems. In: Taylor, H.P., O'Neil, J.R., Kaplan, I.R. (Eds.), Stable Isotope Geochemistry: A Tribute to Samuel Epstein, Special Publication No. 3. The Geochemical Society, San Antonio, Texas, pp. 159–168.

Gat, J.R., Levy, 1978. Isotope hydrology of inland sabkhas in the Bardawil area, Sinai. Limnol. Oceanogr. 23, 841–850.

Gibson, J.J., 2001. Forest-tundra water balance signals traced by isotopic enrichment in lakes. J. Hydrol. 251, 1–13.

Gibson, J.J., 2002. Short-term evaporation and water budget comparisons in shallow arctic lakes using non-steady isotope mass balance. J. Hydrol. 264, 247–266.

Gibson, J.J., Edwards, T.W.D., 2002. Regional surface water balance and evaporation–transpiration partitioning from a stable isotope survey of lakes in northern Canada. Global Biogeochem. Cycles 16 (2). http://dx.doi.org/10.1029/2001GB001839.

Gibson, J.J., Reid, B., 2010. Stable isotope fingerprint of open-water evaporation losses and effective drainage area fluctuations in a subarctic Shield watershed. J. Hydrol. 381, 142–150.

Gibson, J.J., Edwards, T.W.D., Bursey, G.G., Prowse, T.D., 1993. Estimating evaporation using stable isotopes: quantitative results and sensitivity analysis for two catchments in northern Canada. Nord. Hydrol. 24, 79–94.

Gibson, J.J., Edwards, T.W.D., Prowse, T.D., 1996. Development and validation of an isotopic method for estimating lake evaporation. Hydrol. Process. 10, 1369–1382.

Gibson, J.J., Reid, R., Spence, C., 1998. A six-year isotopic record of lake evaporation in the Canadian subarctic: results and validation. Hydrol. Process. 12, 1779–1792.

Gibson, J.J., Edwards, T.W.D., Birks, S.J., St. Amour, N.A., Buhay, W., McEachern, P., Wolfe, B.B., Peters, D.L., 2005. Progress in isotope tracer hydrology in Canada. Hydrol. Process. 19, 303–327.

Gibson, J.J., Birks, S.J., Edwards, T.W.D., 2008. Global prediction of δA and δ^2H–$\delta^{18}O$ evaporation slopes for lakes and soil water accounting for seasonality. Global Biogeochem. Cycles 22, GB2031. http://dx.doi.org/10.1029/2007GB002997.

Gibson, J.J., Birks, S.J., Jeffries, D.S., Kumar, S., Scott, K.A., Aherne, J., Shaw, P., 2010. Site-specific estimates of water yield applied in regional acid sensitivity surveys in western Canada. J. Limnol. 69 (Suppl. 1), 67–76. http://dx.doi.org/10.3274/JL10-69-S1-08.

Gonfiantini, R., 1986. Environmental isotopes in lake studies. In: Fritz, P., Fontes, J.Ch. (Eds.), Handbook of Environmental Isotope Geochemistry, vol. 3. Elsevier, New York, pp. 113–168.

Horita, J., Wesolowski, D., 1994. Liquid–vapour fractionation of oxygen and hydrogen isotopes of water from the freezing to the critical temperature. Geochim. Cosmochim. Acta 58, 3425–3437. http://dx.doi.org/10.1016/0016-7037(94)90096-5.

Horita, J., Rozanski, K., Cohen, S., 2008. Isotope effects in the evaporation of water: a status report of the Craig-Gordon model. Isotopes Environ. Health Stud. 44, 23–49.

Hostetler, S.W., Benson, L.V., 1994. Stable isotopes of oxygen and hydrogen in the Truckee River–Pyramid Lake surface-water system. 2 A predictive model of $\delta^{18}O$ and δ^2H in Pyramid Lake. Limnol. Oceanogr. 39 (2), 356–364.

Ichiyanagi, K., Sugimoto, A., Kurita, N., Ishii, Y., Ohata, T., 2003. Seasonal variation in stable isotopic composition of alas lake water near Yakutsk, Eastern Siberia. Geochem. J. 37, 519–530.

Jasechko, S., Sharp, Z.D., Gibson, J.J., Birks, S.J., Yi, Y., Fawcett, P.J., 2013. Terrestrial water fluxes dominated by transpiration. Nature 496, 347–350.

Kane, D.L., Yang, D., 2004. Overview of water balance determinations for high latitude watersheds. In: Kane, D.L., Yang, D. (Eds.), Northern Research Basins Water Balance, International Association of Hydrological Sciences, vol. 290. IAHS-AISH Publication, pp. 1–12.

Leng, M.J., Anderson, N.J., 2003. Isotopic variation in modern lake waters from western Greenland. Holocene 13 (4), 605–611.

Leng, M.J., Marshall, J.D., 2004. Palaeoclimate interpretation of stable isotope data from lake sediment archives. Quatern. Sci. Rev. 23, 811–831.

Lewis, S., 1979. Environmental isotope balance of Lake Kinneret as a tool in evaporation rate estimations. In: Isotopes in Lake Studies. IAEA, Vienna, pp. 33–65.

Longinelli, A., Stenni, B., Genoni, L., Flora, O., Defrancesco, C., Pellegrini, G., 2008. A stable isotope study of the Garda lake, northern Italy: its hydrological balance. J. Hydrol. 360, 103–116.

Lyon, S.W., Nathanson, M., Spans, A., Grabs, T., Laudon, H., Temnerud, J., Bishop, K.H., Seibert, J., 2012. Specific discharge variability in a boreal landscape. Water Resour. Res. 48, W08506. http://dx.doi.org/10.1029/2011WR011073.

McNaughton, K.G., 1976. Evaporation and advection: evaporation downwind of a boundary separating regions having different resistances and available energies. Q. J. Roy. Meteorol. Soc. 102, 193–202.

Ombradovic, M.M., Sklash, M.G., 1986. An isotopic and geochemical study of the snowmelt runoff in a small arctic watershed. Hydrol. Process. 1, 15–30.

Reid, B., Faria, D., 2004. Evaporation studies in small NWT watersheds. In: Kane, D.L., Yang, D. (Eds.), Northern Research Basins Water Balance, International Association of Hydrological Sciences, vol. 290. IAHS-AISH Publication, pp. 178–185.

Sacks, L.A., 2002. Estimating Ground-water Inflow to Lakes in Central Florida using the Isotope Mass-balance Approach. Water-Resources Investigations Report 02-4192, United States Geological Survey, 59 pp.

Sauer, P.E., Miller, G.H., Overpeck, J.T., 2001. Oxygen isotope ratios of organic matter in arctic lakes as a paleoclimate proxy: field and laboratory investigations. J. Paleolimnol. 25, 43–64.

Soranno, P.A., Webster, K.E., Riera, J.L., Kratz, T.K., Baron, J.S., Bukaveckas, P.A., King, G.W., White, D.S., Caine, N., Lathrop, R.C., Leavitt, R., 1999. Spatial variation among lakes within landscapes: ecological organization along lake chains. Ecosystems 2, 395–410.

Spence, C., Guan, X.J., Phillips, R., Hedstrom, N., Granger, R., Reid, B., 2010. Storage dynamics and streamflow in a catchment with a variable contributing area. Hydrol. Process. 24, 2209–2221.

St. Amour, N.A., Hammarlund, D., Edwards, T.W.D., Wolfe, B.B., 2010. New insights into Holocene atmospheric circulation dynamics in central Scandinavia inferred from oxygen-isotope records of lake-sediment cellulose. Boreas 39, 770–782.

Tondu, J.M.E., Turner, K.W., Wolfe, B.B., Hall, R.I., Edwards, T.W.D., McDonald, I., 2013. Using water isotope tracers to develop the hydrological component of a long-term aquatic ecosystem monitoring program for a northern lake-rich landscape. Arct. Antarct. Alp. Res. 45, 594–614.

Turner, K.W., Wolfe, B.B., Edwards, T.W.D., 2010. Characterizing the role of hydrological processes on lake water balances in the Old Crow Flats, Yukon Territory, Canada, using water isotope tracers. J. Hydrol. 386, 103–117.

Tyler, J.J., Leng, M.J., Arrowsmith, C., 2007. Seasonality and the isotope hydrology of Lochnagar, a Scottish mountain lake: implications for palaeoclimate research. Holocene 17 (6), 717–727.

Wolfe, B.B., Falcone, M.D., Clogg-Wright, K.P., Mongeon, C.L., Yi, Y., Brock, B.E., St. Amour, N.A., Mark, W.A., Edwards, T.W.D., 2007. Progress in isotope paleohydrology using lake sediment cellulose. J. Paleolimnol. 37, 221–231.

Yi, Y., Brock, B.E., Falcone, M.D., Wolfe, B.B., Edwards, T.W.D., 2008. A coupled isotope tracer method to characterize input water to lakes. J. Hydrol. 350, 1–13.

Zimmerman, U., 1979. Determination by stable isotopes of underground inflow and outflow and evaporation of young artificial groundwater lakes. Isotopes in Lake Studies. IAEA, Vienna Austria, pp. 87–94.